An elastic plastic damage formulation for the behavior of concrete

L. Jason* & G. Pijaudier-Cabot
Institut de Recherches en Génie Civil et Mécanique (GéM), Nantes, France
* also at EDF R&D, Clamart, France

A. Huerta
Laboratori de Cacul Numeric, UPC, Barcelona, Spain

R. Crouch
Department of Civil & Structural Engineering, University of Sheffield, England

S. Ghavamian
EDF R&D, Clamart, France

ABSTRACT: Elastic damage models or elastic plastic constitutive laws are not totally sufficient to describe the behavior of concrete. They indeed fail to reproduce the unloading slopes during cyclic loads which define experimentally the value of the damage in the material. When coupled effects are considered in particular in hydromechanical problems, the capability of the numerical model to reproduce the unloading behavior is essential, as an accurate value of the damage is needed. An elastic plastic damage formulation is so proposed and applied to three types of loading : simple tension, cyclic compression and triaxial tests with confinement pressures. It is shown how the plastic part of the model is responsible for the irreversible strains while the damage part simulates the softening behavior.

Keywords: plastic, damage, model, concrete

1 INTRODUCTION

Elastic damage models or elastic plastic laws are not totally sufficient to correctly capture the constitutive behavior of concrete. In some cases (using damage mechanics), the calculation of the damage variable (isotropic case) or tensor (anisotropic laws) is a key point. It can become essential when coupled effects are considered (coupling between damage and permeability, damage and porosity …). In (Picandet et al, 2001) (see figure 1), an experimental law is so proposed between the damage distribution in the material and its gas permeability. Damage is measured using the unloading slope during cyclic compressive loading. In this case, the capability of the constitutive model to capture the unloading behavior is thus essential if a proper evaluation of the permeability needs to be achieved.

An elastic damage model is not appropriate as irreversible strains cannot be captured: a zero stress corresponds to a zero strain and the value of the damage is thus overestimated (figure 2a). An elastic plastic relation is not adapted (even with softening, see for example Grassl et al, 2002) as the unloading curve follows the elastic slope (figure 2b). Another alternative consists in combining these two approaches to propose an elastic plastic damage law. The softening behavior and the decrease in the elastic modulus are so reproduced by the damage part while the plasticity effect accounts for the irreversible strains. With this formulation, experimental unloading can be simulated correctly (figure 2c).
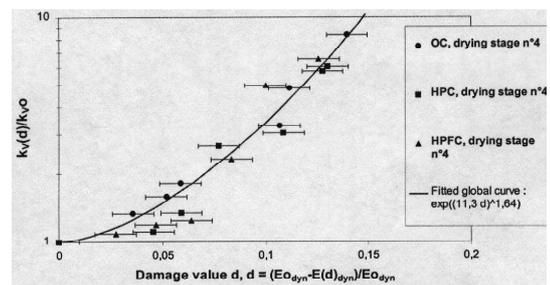

Figure 1. Experimental relation between damage and permeability. k_{v0} and k_v are the intrinsic permeabilities of the initial and damaged material respectively. (Picandet et al, 2001).

It is such a model which is presented in this contribution. The constitutive law is validated on three different applications : a simple tension test to evaluate the ability of the simulation to capture

the softening behavior of concrete, a cyclic compressive loading to reproduce the development of irreversible strains, and a triaxial test with confinement to study the material response with increasing hydrostatic pressures. For each loading, the plastic damage simulation is compared with experimental results and with an elastic damage formulation to underline the interest of including "plastic" strains.
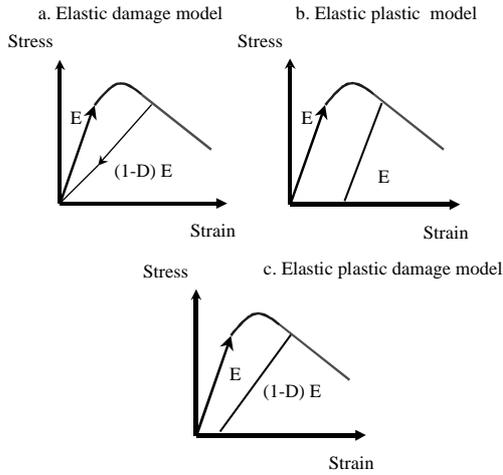

Figure 2. Unloading response of elastic damage, elastic plastic and elastic plastic damage models.

2 MODEL FORMULATION

2.1 *Plasticity*

The plastic model is governed by the following set of equations :

$$
\begin{aligned}
d\varepsilon &= d\varepsilon^e + d\varepsilon^p \quad \text{(total strain decomposition)} \\
\sigma' &= E\varepsilon^e \quad\quad \text{(elastic relation)} \\
\dot{\varepsilon}^p &= \dot{\lambda} m(\sigma', k_h) \quad \text{(flow equations)} \\
\dot{k}_h &= \dot{\lambda} h(\sigma', k_h)
\end{aligned} \tag{1}
$$

where ε, ε^e and ε^p are respectively the total, elastic and plastic strains, σ' is the effective stress, E is the elastic tensor, λ the plastic multiplier and k_h the hardening parameter ($0 \leq k_h \leq 1$). m and h are the flow vectors defined by :

$$
m = \frac{\partial f}{\partial \sigma}
$$

$$
h = \frac{\sqrt{\frac{2}{3}\frac{\partial f}{\partial \sigma}:\frac{\partial f}{\partial \sigma}}}{\varsigma(\sigma)} \tag{2}
$$

where f is the yield surface and ζ a function of the stress (Etse et al, 1994).

$$
f = \overline{\rho}^2 (J_2) - \frac{k(k_h, I_1)\overline{\rho_c}^2(I_1)}{r^2(\theta, I_1)} \tag{3}
$$

with I_1 and J_2 the stress invariant and θ the Lode angle function of the second and third stress invariant and ranging from [$-\pi/6$; $\pi/6$]. $k, \overline{\rho_c}$ and r are three functions of the stress invariant and internal variable.

$$
\overline{\rho} = \frac{\sqrt{2J_2}}{r_c}, \ \overline{\xi} = \frac{I_1}{\sqrt{3}r_c} \tag{4}
$$

where r_c is a parameter.

The evolution of the plastic multiplier is finally given by :

$$
f(\sigma', k_h) \leq 0, \quad \dot{\lambda} \geq 0, \quad f(\sigma', k_h)\dot{\lambda} = 0 \tag{5}
$$

This local problem is solved with an iterative procedure associated to a closest point projection algorithm (see Perez-Foguet et al, 2000).

Figure 3 shows the evolution of the yield surface with an increasing hardening parameter k_h for simple compression. Figure 4 highlights the non symmetry of the plastic surface with the Lode angle (for simple compression, simple tension or hydrostatic loading).
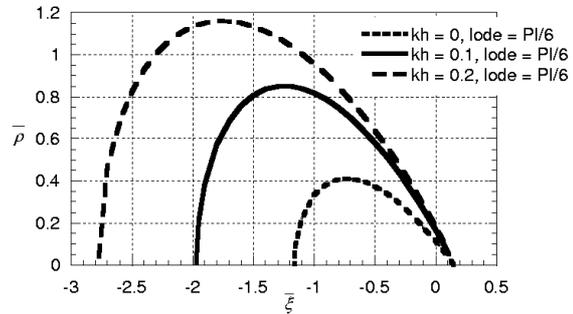

Figure 3. Plastic yield surface. Evolution with the hardening parameter for simple compression (Lode = PI/6).
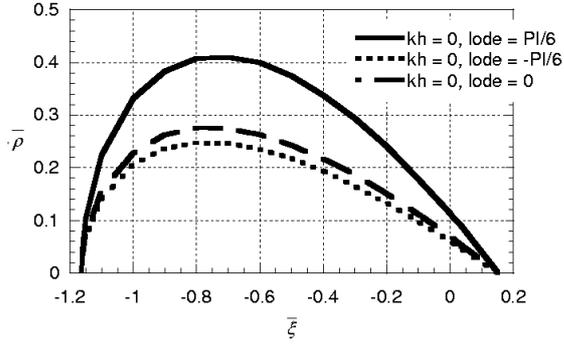
Figure 4. Plastic yield surface. Evolution with Lode angle (simple compression, lode = PI/6, simple tension, lode = -Pi/6, hydrostatic loading, lode = 0).
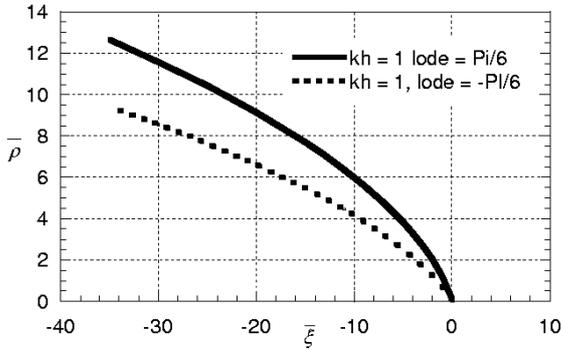

Figure 5. Plastic yield surface. Failure surface for an hardening parameter equal to 1.

Depending on the type of loading which is applied, the initial threshold (and the evolution) of plasticity is not the same. Finally, figure 5 illustrates the failure surfaces for simple tension and compression. As the hardening parameter has a limited value of 1, once it has reached this critical level, hardening is not allowed any more and the yield surface becomes a failure one (constant effective stress).

2.2 *Damage model*

The damage part of the model was initially developed in (Mazars, 1984). It describes the constitutive behavior of concrete by introducing a scalar variable D that quantifies the influence of microcracking.

For the description of the damage growth, an equivalent strain ε_{eq} is introduced from the elastic strain tensor ε^e.

$$\varepsilon^e = C^{-1}\sigma' \qquad (6)$$

where C^{-1} is the inverse of the elastic tensor.

$$\varepsilon_{eq} = \sqrt{\sum_{i=1}^{3}(<\varepsilon_i^e>_+)^2} \qquad (7)$$

with $<\varepsilon_i^e>_+$ the positive principal elastic strains.

The loading surface g is defined by:

$$g(\varepsilon^e, D) = \tilde{d}(\varepsilon^e) - D \qquad (8)$$

where the damage variable D is also the history variable which takes the maximum value reached by $\tilde{d}$ during the history of loading, $D = Max_{/t}(\tilde{d}, 0)$

$\tilde{d}$ is defined by an evolution law which distinguishes the mechanical responses of the material in tension and in compression with the help of two couples of scalars, (α_t, D_t) for tension and (α_c, D_c) for compression.

$$\tilde{d}(\varepsilon^e) = \alpha_t(\varepsilon^e)D_t(\varepsilon_{eq}) + \alpha_c(\varepsilon^e)D_c(\varepsilon_{eq})$$

$$D_{t,c} = 1 - \frac{\varepsilon_{D0}(1 - A_{t,c})}{\varepsilon_{eq}} - \frac{A_{t,c}}{\exp[B_{t,c}(\varepsilon_{eq} - \varepsilon_{D0})]} \qquad (9)$$

$$\alpha_{t,c} = \left(\sum_{i=1}^{3}\frac{<\varepsilon_i^{t,c}><\varepsilon_i^{el}>_+}{\varepsilon_{eq}^2}\right)$$

ε_{D0} is a parameter and represents the initial threshold from which damage grows. D_t and D_c are the tensile and compressive parts of the damage. A_t, A_c, B_t and B_c are four parameters. The weights α_t and α_c are computed from the elastic strain tensor. They are defined as functions of the principal values of the strains ε_i^t and ε_i^c due to positive and negative effective stresses. In uniaxial tension, $\alpha_t = 1$ and $\alpha_c = 0$. In uniaxial compression, $\alpha_t = 0$ and $\alpha_c = 1$.

The evolution of damage is determined by the Kuhn – Tucker conditions :

$$g \leq 0, \quad \dot{\tilde{d}} \geq 0, \quad g\dot{\tilde{d}} = 0 \qquad (10)$$

Once the damage variable has been calculated, the stress is computed :

$$\sigma = (1-D)\sigma' \qquad (11)$$

2.3 *Model implementation*

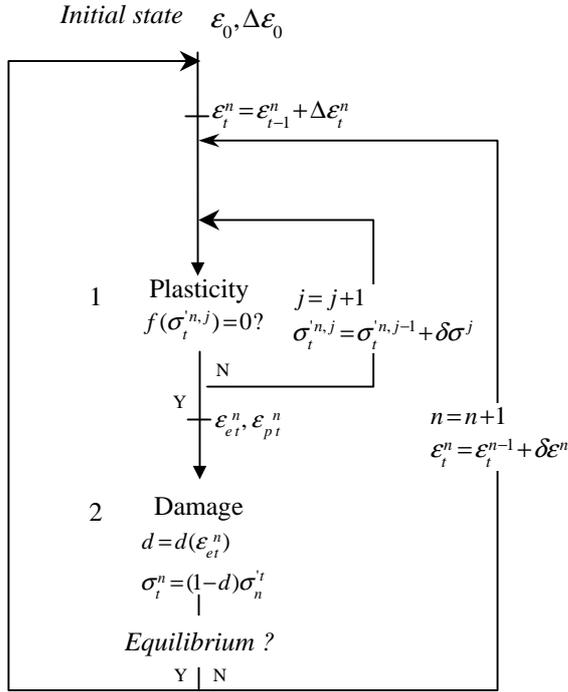The integration of the constitutive law follows two main steps as depicted in figure 6.

Initial state $\varepsilon_0, \Delta\varepsilon_0$

$$\varepsilon_t^n = \varepsilon_{t-1}^n + \Delta\varepsilon_t^n$$

1 Plasticity $\quad j = j+1$
$f(\sigma_t'^{n,j}) = 0?$ $\quad \sigma_t'^{n,j} = \sigma_t'^{n,j-1} + \delta\sigma^j$

N

Y $\quad \varepsilon_{et}^n, \varepsilon_{pt}^n$ $\qquad n = n+1$
$$\varepsilon_t^n = \varepsilon_t^{n-1} + \delta\varepsilon^n$$

2 Damage
$d = d(\varepsilon_{et}^n)$
$\sigma_t^n = (1-d)\sigma_n'^t$

Equilibrium ?

Y | N

Figure 6. Elastic plastic damage formulation. Principle of the computational implementation.

The state at time t-1 (i.e. quantities ε_{t-1} and σ_{t-1}) and the total strains ε_t^n at time t and global iteration n are known. An effective stress $\sigma'^{n,j}_t$ (undamaged stress) is then computed using the equations of plasticity (particularly the expression of the yield surface f) (step 1) (see section 2.1.). After an initial prediction, successive corrections, $\delta\sigma^j$, are applied, if necessary, to determine the appropriate value of the effective stress. Once the elastic – plastic strain decomposition $\varepsilon_{e,t}^{\ n}$ $\varepsilon_{p,t}^{\ n}$ is known (from the plasticity), a scalar damage variable D is calculated. Finally, the total stress σ_t^n is computed from the damage and the effective stress. If the equilibrium equations of the mechanical problem are not satisfied, some corrections $\delta\varepsilon^n$ are considered on the total strains (Newton – Raphson iterative scheme).

3 VALIDATION

The constitutive law is now going to be validated on three types of loading : a simple tension test, a cyclic compression and a triaxial application with increasing confinement pressures.

3.1 Simple tension test

For concrete, tension is the most relevant loading that a model has to predict as far as cracking is concerned. It is indeed when the concrete is subjected to tension that the first cracks usually appear.

That is why the numerical response (elastic plastic damage law) is first compared with such a test (Gopalaratnam et al., 1985). Figure 7 gives the axial stress – strain curve. To evaluate the interest of including plasticity in the formulation, a pure damage model is also considered for which the plastic strains are supposed to keep a constant zero value so as the elastic strain equals exactly the total strain ($\varepsilon = \varepsilon^e$) (original damage model, Mazars,1984). Figure 8 illustrates the simulation with the elastic damage model. As the development of damage is predominant during simple tension tests, the two models are able to reproduce the experiment globally. Especially, the elastic plastic damage constitutive law gives a correct value of the peak position and simulates the post peak behavior. Choosing the appropriate parameters, the model is thus adapted for simple tension test.
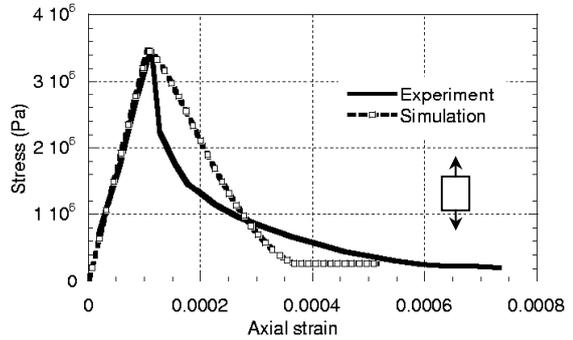
Figure 7. Stress strain curve for simple tension test. Elastic plastic damage formulation.
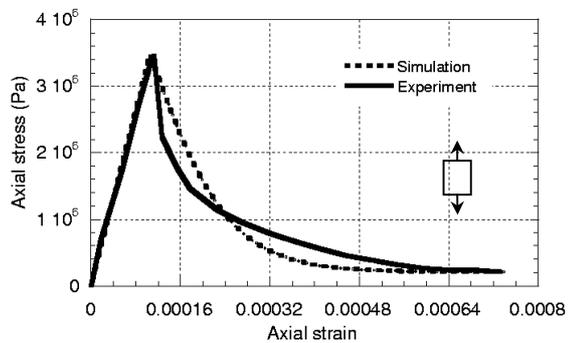
Figure 8. Stress strain curve for simple tension test. Elastic damage constitutive law.

3.2 Cyclic compression simulation

Cyclic compression is the second elementary test used to validate the interest of the model. Experimental results are taken from (Sinha et al, 1964). Figure 9 illustrates the numerical response for simple damage law (without plasticity). With this type of relation, a zero stress corresponds to a zero strain. No irreversible effect is simulated. The unloading curve is elastic with a slope equal to the damaged Young's modulus E_d .

$$E_d = (1-D)E_0 \qquad (12)$$

with E_0 the virgin Young's modulus.

The numerical response of the elastic plastic damage model is given in figure 10. This time, damage induces the global softening behavior of concrete while the plastic part reproduces quantitatively the evolution of the irreversible strains. Experimental and numerical unloading slopes are thus similar, contrary to the simple damage formulation response.

If this difference could seem negligible, it is in fact essential if a correct value of the damage needs to be captured. The elastic damage model overestimates D whereas the full constitutive law provides more acceptable results.

Figures 11 and 12 illustrate the differences between the two approaches in term of volumetric behaviors. While, with the simple damage law, the volumetric strains keep negative values, the introduction of plasticity simulates a change in the volumetric response from contractant (negative volumetric strains) to dilatant, a phenomenon which is experimentally observed (see Sfer et al, 2002 for example).

The introduction of plasticity associated with the development of damage plays thus a key role in the numerical simulation of a cyclic compression test.
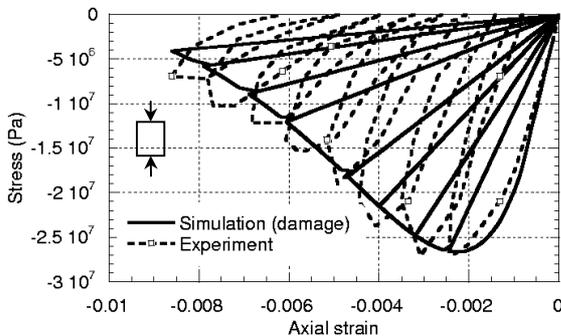

Figure 9. Cyclic compression test. Elastic damage simulation.
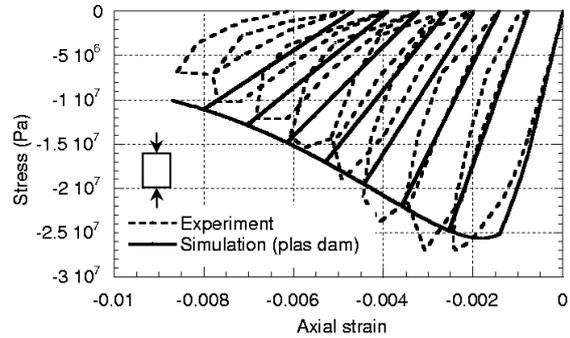

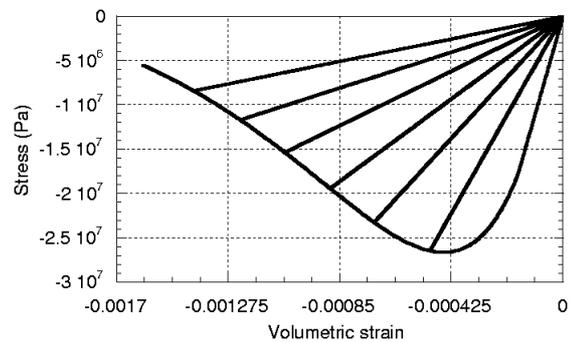Figure 10. Cyclic compression test. Elastic plastic damage formulation.

Figure 11. Cyclic compression test. Volumetric behavior for elastic damage model.
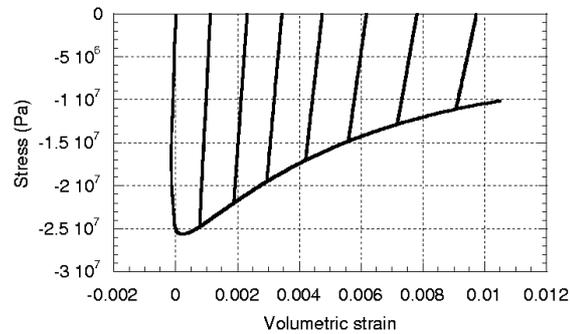

Figure 12. Cyclic compression test. Volumetric behavior for elastic plastic damage model.

The apparition of irreversible strains during loading is quantitatively reproduced and the softening behavior fits well. Moreover, the volumetric response, that was totally misevaluated by the elastic damage model, is correctly simulated by the full formulation.

3.3 Triaxial test with confinement pressures

To evaluate the ability of the constitutive law to reproduce triaxial tests after hydrostatic loading,

the experimental results from (Sfer et al, 2002) are simulated.

A vertical displacement is applied on the plane face of a concrete cylinder after an initial hydrostatic loading.

Numerical results are compared with experiment for different levels of confinement pressures (P = 0, 1.5, 4.5, 9, 30 and 60 MPa). Figure 13 gives the axial response after the confinement phase (the application of the hydrostatic pressure is not represented) for the first four pressures.

Simulations and experiment propose similar results. The peak position is quantitatively well reproduced (except for 1.5 MPa). The global evolution is also correct: the maximum of the axial stress increases with the pressure and the softening part is less and less significant. When the initial hydrostatic pressure takes higher values, the damage part of the model plays a minor role and plasticity effect becomes predominant.
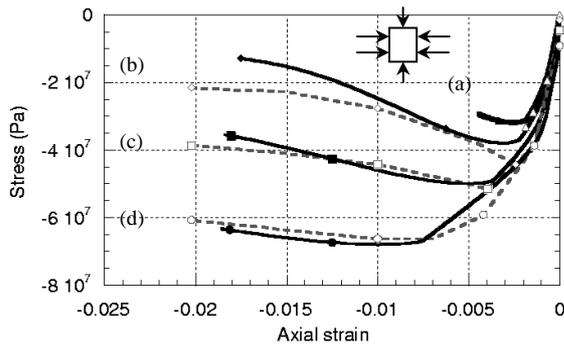

Figure 13. Triaxial test with increasing confinement. Axial stress - strain curves for low hydrostatic pressures. Straight lines (black markers) correspond to simulation, dotted lines (white markers) to experiment.
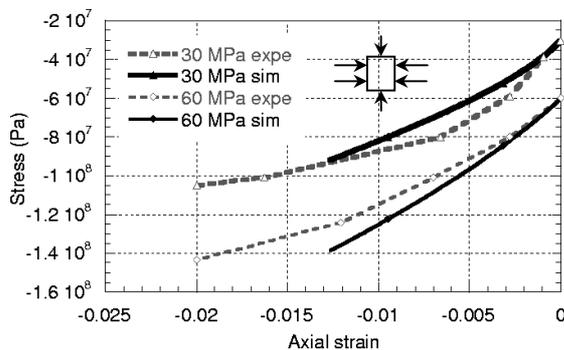(a) 0 MPa, (b) 1.5 MPa, (c) 4.5 MPa, (d) 9 MPa

Figure 14. Triaxial test with increasing confinement. Axial stress – strain curves for high hydrostatic pressures.
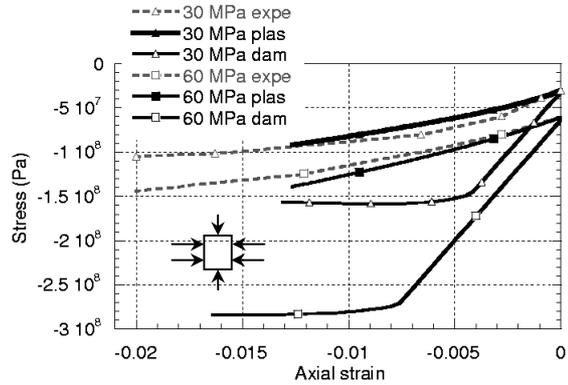

Figure 15. Triaxial test with increasing confinement. Axial stress strain curves for high hydrostatic pressures. Comparison between the elastic damage model (dam) and the elastic plastic damage formulation (plas).
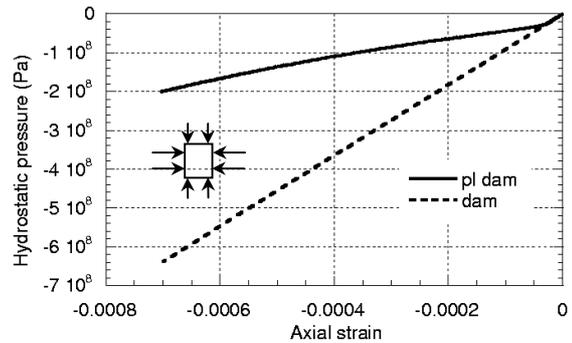

Figure 16. Hydrostatic confinement. Comparison between elasic plastic damage model (pl dam) and elastic damage constitutive law (dam).

Figure 14 presents the axial curves for 30 and 60 MPa. Once again, experimental results and simulations are in agreement. Especially, the decrease in the initial modulus is reproduced by the consitutive law.

Figure 15 proposes a comparison between the elastic plastic damage formulation and the damage model for the high confinement pressures. The damage law fails to reproduce the decrease in the initial modulus. As soon as the pressure takes important values (30 MPa and 60 MPa in the figure), the model gives an overestimated prevision of the real behavior. In fact, this comes from the definition of the equivalent strain (7) that characterizes the material extension during loading. When the hydrostatic pressure is applied, the sample is not subjected to tension, the equivalent strain keeps a zero value and the material response is elastic. If this prediction is acceptable for low confinement pressures, it is no longer true when one considers higher levels. For 30 MPa for

example, non linearity has already initiated when the application of the vertical displacement begins. On the contrary, the introduction of plasticity and the characteristic shape of the associated yield surface (closed function along the volumetric invariant) enable to simulate the non linear behavior. To underline this difference, figure 16 gives the two stress strain curves during the application of the hydrostatic pressures. As expected, the elastic damage evolution is linear whereas with the elastic plastic damage model, a decrease in the slope is observed.

Figure 17 shows the evolution of the simulated transversal strains for low confinement pressures and a comparison with experiment. Even if the first part of the curve is underestimated by the simulation, the transversal strains are globally correct.
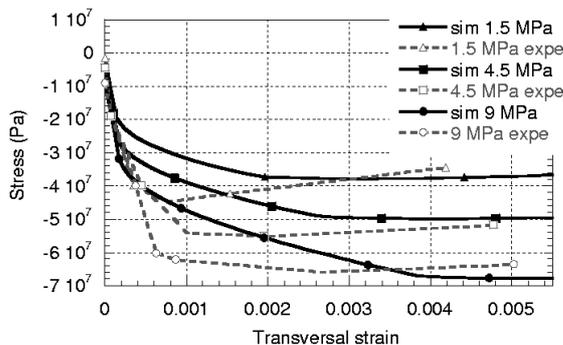

Figure 17. Triaxial test with increasing confinement. Axial stress vs transversal strains for 1.5, 4.5 and 9 MPa.

4 CONCLUSIONS

An elastic plastic damage formulation was developed to simulate the response of concrete under different loading. It is based on an isotropic damage model, for the description of the softening behavior and the degradation of the Young's modulus which is associated to a plastic surface, responsible for the irreversible strains. The constitutive law was tested on three applications.

For simple tension, where damage is predominant compared to plasticity, the response was correctly described. Especially the peak position and the post peak part were simulated in a good way.

Cyclic compression underlines the necessity to include a plastic surface. If the softening part is reproduced by both elastic damage and elastic plastic damage models, only the second one is able to simulate the development of irreversible strains. With this formulation, unloading slopes are in agreement with experimental results. A "plastic" effect is also observed on the volumetric behavior with a characteristic change from a contractant response to a dilatant response.

Finally, triaxial confinement tests confirm the interest of the association of damage and plasticity. The experimental evolution of the peak stress and the softening part with increasing hydrostatic pressures are noticed especially. Due to its shape, the plastic yield surface is able to simulate the decrease of the initial slope observed for some levels of confinement. The experimental transversal strains are also reproduced.

5 ACKNOWLEDGMENTS

6 REFERENCES

Etse, G. Willam, K. 1994. Fracture energy formulation for inelastic behavior of plain concrete. *Journal of engineering mechanics (ASCE)* 120 1983-2011

Gopalaratnam, V.S. Shah, S.P. 1985. Softening response of plain concrete in direct tension. *ACI Journal* May-June 1985, 310-323.

Grassl, P. Lundgren, K. Gylltoft, K. 2002. Concrete in compression: a plasticity theory with a novel hardening law. *International Journal of Solids and Structures* 39:5205-5223.

Mazars, J. 1984. Application de la mécanique de l'endommagement au comportement non linéaire et à la rupture du béton de structure, *PhD Thesis,* Université Paris VI.

Perez-Foguet, A. Rodriguez-Ferran, A. Huerta, A. Numerical differentiation for non trivial consistent tangent matrices: an applicationto the MRS-Lade model, *International journal for numerical methods in engineering,* 48:159-184

Picandet, V. Khelidj, A. Bastian, G. 2001. Effect of axial compressive damage on gas permeability of ordinary and high-performance concrete. *Cement and Concrete Research*, 31 1525-1532.

Sfer, D. Carol, I. Gettu, R. Etse, G. 2002. Study of the behavior of concrete under triaxial compression. *Journal of engineering mechanics* 128 2 156-163

Simo, J.C. Hugues, T.J.R. 1998. Computational inelasticity. Springer Verlag.

Sinha, B.P. Gerstle, K.H. Tulin, L.G. 1964. Stress strain relations for concrete under cyclic loading. *Journal of the American concrete institute* February 1964 195-211